2020 IEEE 9th International Power Electronics and Motion Control Conference (IPEMC2020-ECCE Asia) | 978-1-7281-5301-8/20/$31.00 ©2020 IEEE | DOI: 10.1109/IPEMC-ECCEAsia48364.2020.9367680

Fixed Switching Frequency Predictive Control for PMSM Drives With Guaranteed Control Dynamics

Xiaodong Liu, Zhenbin Zhang*, Xinliang Yang
School of Electrical Engineering
Shandong University
Jinan 250061, China
zbz@sdu.edu.cn

Cristian Garcia, José Rodríguez
Facultad de Ingenieria
Universidad Andres Bello Chile
Santiago 8370146, Chile
jose.rodriguez@unab.cl

***Abstract*—In this work, we propose a switched direct model predictive control (DMPC) method for permanent magnet synchronous motor (PMSM) drives; it achieves a fixed switching frequency while preserving fast control dynamics of the DMPC technique. In steady-state operation, the predictive period control (PPC) approach is adopted to carry out fixed switching frequency operation. Meanwhile, during transients, the classical DMPC (CDMPC) method is used to provide fast control dynamics. Furthermore, the criteria to switch between the two modes are presented in detail; these criteria ensure a smooth transition. The proposed method has been verified using a PMSM drive fed by a two-level (2L) voltage source converter. The simulation results confirm its effectiveness.**

***Index Terms*—Direct model predictive control, Fixed switching frequency, PMSM drives**

I. Introduction

With the rapid development of the more powerful microprocessor, direct model predictive control has emerged as a promising alternative for power electronics and motor drives [1], [2]. DMPC uses the available system model to predict the motor's future behavior for a finite set of control actions, i.e., different voltage vectors of the power converter. Then it selects the optimal voltage vector that minimizes the predefined cost function, and applies the chosen one for the whole control interval (t_c). The aforementioned procedure is repeated with new measurements at every sampling instant. DMPC is characterized by its straightforward concept, flexibility in design and fast dynamics [3]. However, the switching frequency (f_{sw}) of DMPC is unfixed due to its lack of modulator. This leads to a widely spread voltage and current spectrum, which in turn gives rise to iron and copper losses of motor [4] and may induce undesirable resonance oscillation, posing risk to the motor's normal operation [5]. Furthermore, the maximum switching frequency can reach half of the sampling frequency theoretically, which means high power losses and low efficiency. In summary, unfixed switching frequency of MPC has been a growing concern.

The corresponding author of this work is Zhenbin Zhang. This work is financially supported in part by the Shandong Provincial Key Research and Development Program (Major Scientic and Technological Innovation Project NO.2019JZZY020805), in part by the National Distinguished Expert (Youth Talent) Program of China (31390089963058), in part by the General Program of National Natural Science Foundation of China (51977124), in part by the Shandong Natural Science Foundation (ZR2019QEE001). J. Rodriguez acknowledges the support of ANID through projects FB0008, ACT192013 and 1170167.

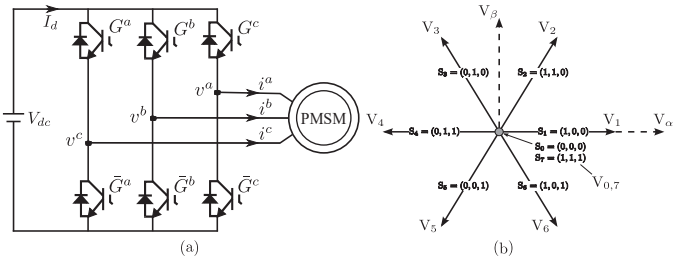

Fig. 1. (a) Power circuit of the two-level power converter driving the PMSM system. (b) Eight vectors generated by 2L converters.

Methods to address such issues can be classified into two categories, i.e., modulation-based and non-modulation-based solutions. The former set synthesizes basic voltage vectors during one control interval [6]–[8]. However, the power converter's switching nature is not fully considered. The latter set includes techniques such as simple switching effort penalization to limit the switching frequency [9], notch filter to reduce the harmonics at specific frequencies [10] and predefined sliding window, for which a certain number of switching process shall occur [11], etc. Nevertheless, the spectrum achieved by this latter set is unsatisfactory, compared with the results attained through the use of modulators. In [12], [13], by including the switching period term into the cost function, a simple predictive period control approach is presented. The control structure of DMPC is preserved, while the controlled currents exhibit modulation-like harmonic spectra. However, a deteriorated transient performance is observed for motor control (see Sec. IV-A), which weakens the positive feature of DMPC.

Inspired by the above analysis, we propose a novel switched DMPC method, which combines the advantages of predictive period control, in terms of fixed switching frequency, and classical DMPC, in terms of fast control dynamics. Permanent-magnet synchronous motor (PMSM) shows attractive properties, e.g., higher energy density, wider speed range, reduced maintenance and easy to control, etc [14]. PMSM fed by 2L power converter system is selected as a case study. The

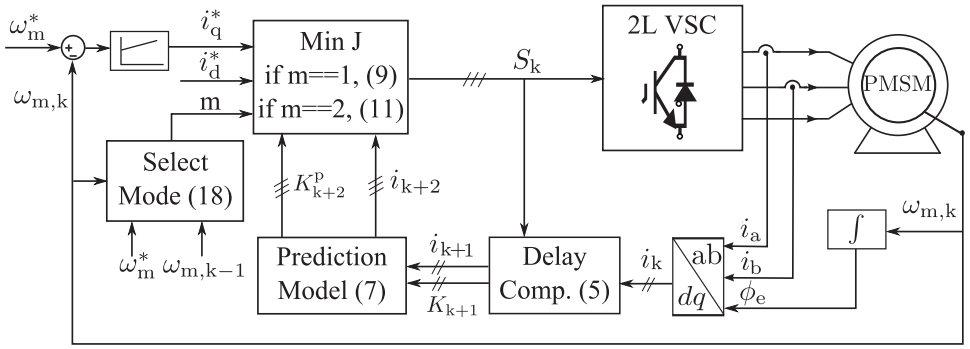

Fig. 2. Overall control diagram of the switched DMPC. Classical DMPC is used when m=1. And PPC technique is applied when m=2.

contributions, indexed to the following sections, include:

(i) DMPC with a predictive period control approach is extended from its simple application for RL load control to PMSM motor drives, achieving fixed switching frequency operation and modulation-like control variable spectrum (See Sec. IV-C);

(ii) We closely investigate the reasons for the reduced transient control capability of the PPC method (See Sec. IV-A), and propose a switched DMPC method to solve such issues (See Sec. III);

(iii) The criteria using the hysteresis band to distinguish between the transient and steady-state operation modes of the PMSM drives is given to achieve a smooth switch between the two control laws, thus avoiding chatter problem (See Sec. III-C).

II. System Description and Modeling

In this section, the control target – the 2L power converter-fed PMSM shown in Fig. 1a is described. The variables in the rotating (dq) frame is obtained utilizing the (power-invariant) Park-Transformation,

$$\mathbf{x}_{\rm dq} = \sqrt{\frac{2}{3}}\begin{bmatrix} \cos(\phi) & \cos(\phi-2\pi/3) & \cos(\phi+2\pi/3) \\ -\sin(\phi) & -\sin(\phi-2\pi/3) & -\sin(\phi+2\pi/3) \end{bmatrix}\mathbf{x}_{\rm abc}, \tag{1}$$

where ϕ is the position of flux vector, $\mathbf{x}_{\rm dq}$ and $\mathbf{x}_{\rm abc}$ denote quantities in dq and abc coordinate. Meanwhile, the system discrete prediction model is derived by applying the forward-Euler formula, considering that the sampling time $T_{\rm s}$ is small enough.

A. Power converter

For $x \in \{a, b, c\}$, G^x denotes the upper IGBT's gate signal, and $\bar{G}^x$ (complementary to G^x) the inverse gate signal for the lower IGBT. The switching state S_x for 2L power converter is described as

$$S_x := \mathcal{G}(G^x) = \begin{cases} 1\ (P) & \text{if}: G^x = 1 \wedge \bar{G}^x = 0 \\ 0\ (N) & \text{if}: G^x = 0 \wedge \bar{G}^x = 1. \end{cases} \tag{2}$$

And the 8 switching states have the following form which are depicted in Fig. 1b.

$$\boldsymbol{S}_{\rm abc} = (S_{\rm a}, S_{\rm b}, S_{\rm c})^\top \in \mathcal{S}_8 := \{NNN, NNP, \cdots, PPP\}. \tag{3}$$

Taking switching states and DC-link voltage $V_{\rm d}$ into consideration, the phase voltages of the converter can be obtained as [15]

$$\begin{bmatrix} v_{\rm a} \\ v_{\rm b} \\ v_{\rm c} \end{bmatrix} = \frac{V_{\rm d}}{3}\begin{bmatrix} 2 & -1 & -1 \\ -1 & 2 & -1 \\ -1 & -1 & 2 \end{bmatrix}\boldsymbol{S}_{\rm abc}. \tag{4}$$

B. PMSM modeling

With regards to the PMSM, the stator currents are taken as state variables to describe its dynamics [15],

$$\mathbf{x}_{\rm k+1} = \mathbf{A}_{\rm k}\mathbf{x}_{\rm k} + \mathbf{B}\mathbf{u}_{\rm k} + \mathbf{H}_{\rm k}, \tag{5}$$

where $\mathbf{x}_{\rm k} = \boldsymbol{i}_{\rm k}^{\rm dq} = (i_{\rm k}^{\rm d}, i_{\rm k}^{\rm q})^\top (\mathrm{A})^2$ is the stator current vector in dq-coordinate, $\mathbf{u}_{\rm k} = \boldsymbol{v}_{\rm k}^{\rm dq} = (\boldsymbol{v}_{\rm k}^{\rm d}, \boldsymbol{v}_{\rm k}^{\rm q})^\top (\mathrm{V})^2$ is the output voltage vector of the converter, and $\mathbf{A}_{\rm k}$, $\mathbf{B}$, $\mathbf{H}_{\rm k}$ are system, input and feed-through matrices, respectively. The components of three matrices can be described as,

$$\mathbf{A}_{\rm k} = \begin{bmatrix} 1-\frac{T_{\rm s}R_{\rm s}}{L_{\rm s}} & T_{\rm s}\omega_{\rm e}(k) \\ -T_{\rm s}\omega_{\rm e}(k) & 1-\frac{T_{\rm s}R_{\rm s}}{L_{\rm s}} \end{bmatrix},\ \mathbf{B} = \begin{bmatrix} \frac{T_{\rm s}}{L_{\rm s}} & 0 \\ 0 & \frac{T_{\rm s}}{L_{\rm s}} \end{bmatrix},$$
$$\mathbf{H}_{\rm k} = \begin{bmatrix} 0 \\ -\frac{T_{\rm s}\psi_{\rm pm}}{L_{\rm s}}\omega_{\rm e}(k) \end{bmatrix}, \tag{6}$$

where $T_{\rm s}$ (s) is the sampling interval, $R_{\rm s}$ (Ω), $L_{\rm s}$ (Vs/A) are stator resistance and inductance, respectively, $\omega_{\rm e}$ (rad/s) denotes the electrical angular speed and $\psi_{\rm pm}$ (Wb) corresponds to permanent-magnet flux linkage. Note that, to compensate for the one-step delay in the digital controller system, a two-step prediction technique is adopted [16]. Stator currents at k+2 instant can be predicted as,

$$\mathbf{x}_{\rm k+2} = \mathbf{A}_{\rm k}\mathbf{x}_{\rm k+1} + \mathbf{B}\mathbf{u}_{\rm k+1} + \mathbf{H}_{\rm k}, \tag{7}$$

where $\mathbf{A}_{\rm k}$ and $\mathbf{H}_{\rm k}$ are assumed to be unchanged, since the time constant of the rotor speed is much slower than the electrical variables.

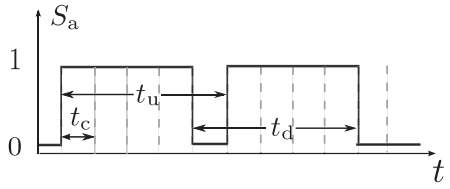

Fig. 3. Switching period between rising or falling edges for one phase gate signal, t_u and t_d respectively. t_c denotes the control interval.

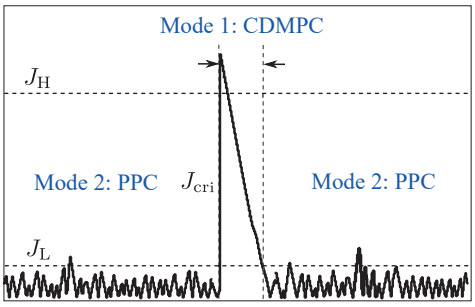

Fig. 4. Mode switch criteria between PPC and CDMPC using a hysteresis band.

III. Switched DMPC

Designing the cost function is a core part of implementing DMPC to realize the desired control performance. In the following section, classical DMPC, PPC (with different cost function designs) and the operating modes' switch criteria are discussed. The overall control diagram is depicted in Fig. 2.

A. Classical DMPC (Mode 1)

In mode 1, current reference tracking and switch effort penalization are mapped into the cost function,

$$J_{\mathrm{i}} = \|\boldsymbol{i}^*_{\mathrm{k+2}} - \boldsymbol{i}_{\mathrm{k+2}}\|^2,\ J_{\mathrm{s}} = \|\boldsymbol{S}_{\mathrm{k+1}} - \boldsymbol{S}_{\mathrm{k}}\|_1, \tag{8}$$

where J_{i} and J_{s} corresponds to the first and second control target, and $\|\boldsymbol{x}\|_1$ and $\|\boldsymbol{x}\|$ denote the 1-norm and 2-norm of the vector $\boldsymbol{x}$, respectively. The cost function for classical DMPC (mode 1) is designed as,

$$J_1 = J_{\mathrm{i}} + \lambda_{\mathrm{s}} J_{\mathrm{s}}, \tag{9}$$

where λ_{s} is the weighting factor to trade off between the current tracking performance and the switching frequency.

B. PPC method (Mode 2)

The basic principle of the PPC method in [12] is briefly reviewed in this section. Switching frequency is defined as the number of switching events that take place in a certain time. For the linear control methods with the modulator, such as carrier-based pulse width modulation (CB-PWM) or space vector modulation (SVM), converter switches change states twice within one control period. Such switching mechanism leads to the fixed switching frequency. Note that $t_{\mathrm{sw}} = t_{\mathrm{c}}$ for classical linear approaches, where t_{sw} denotes the switching period. The situation is different for DMPC. DMPC updates a new voltage vector at every control step without considering the past behavior. The same vector may be considered as optimal for several consecutive control interval. Hence, $t_{\mathrm{sw}} = Q * t_{\mathrm{c}}$, where Q is a *time-varying* integer and $Q \geq 2$. Accordingly, variable f_{sw} is observed in DMPC, similar to other direct control methods, e.g., direct torque control, hysteresis control and sliding mode control.

Different from the speed, current or flux, which are easily predicted using the system model, future switching frequency is difficult to estimate. As a result, the it's difficult to regulate the f_{sw} in the cost function. In [12], instead of regulating the switching frequency directly, the switching period is controlled and added into the cost function to achieve the fixed switching frequency. Imitating the switch mechanism of linear control methods, where $t_{\mathrm{u}} = t_{\mathrm{d}}$ (see Fig. 3), the control target of PPC is set as $t_{\mathrm{u}} = t_{\mathrm{d}} = t^*_{\mathrm{sw}} = \mathrm{K}^* t_{\mathrm{c}}$, where K^*, the so-called *period counts*, denotes the number of control intervals within one switch period. For example, in this work, the control interval is set as $t_{\mathrm{c}} = 1/80$ kHz $= 12.5\mu s$ and the desired switching period is set as $t^*_{\mathrm{sw}} = 1/5\mathrm{kHz} = 200\mu s$, then $\mathrm{K}^* = 16$. The controller regulates the amount of control intervals between up and down periods, i.e., $\mathbf{K}_{\mathrm{u}} = (k_{\mathrm{u,a}},\ k_{\mathrm{u,b}}, k_{\mathrm{u,c}})^\top$ and $\mathbf{K}_{\mathrm{d}} = (k_{\mathrm{d,a}}, k_{\mathrm{d,b}}, k_{\mathrm{d,c}})^\top$, where $k_{\mathrm{u}} = t_{\mathrm{u}}/t_{\mathrm{c}} = t_{\mathrm{d}}/t_{\mathrm{c}}$. This enables the use of integers rather than floating period time in second, which reduces the computational burden. The switching period regulation term is defined as

$$J_{\mathrm{K}} = \|\mathbf{K}^* - \mathbf{K}^{\mathrm{p}}_{\mathrm{u,k+2}}\|^2 + \|\mathbf{K}^* - \mathbf{K}^{\mathrm{p}}_{\mathrm{d,k+2}}\|^2, \tag{10}$$

The cost function for PPC (mode 2) is designed as

$$J_2 = J_i + \lambda_{\mathrm{K}} J_{\mathrm{K}}. \tag{11}$$

The *period counts* update according to the following rules. $\mathbf{K}_{\mathrm{u}}$ and $\mathbf{K}_{\mathrm{d}}$ are increased by 1 if no commutation takes place and reset to 1 when the corresponding up and down commutations occur. The *period counts* provide DMPC with a record of the past switching behavior, which makes controlling f_{sw} possible. $\boldsymbol{S}_{\mathrm{k-1}}\|\bar{\boldsymbol{S}}_{\mathrm{k}}$ and $\bar{\boldsymbol{S}}_{\mathrm{k-1}}\|\boldsymbol{S}_{\mathrm{k}}$ are employed to detect the up and down commutation, respectively. And the period counts at k+1 instant can be estimated as

$$\begin{aligned} \boldsymbol{K}_{\mathrm{u,k+1}} &= \boldsymbol{K}_{\mathrm{u,k}}\ (\boldsymbol{S}_{\mathrm{k-1}}\|\bar{\boldsymbol{S}}_{\mathrm{k}}) + 1, \\ \boldsymbol{K}_{\mathrm{d,k+1}} &= \boldsymbol{K}_{\mathrm{d,k}}\ (\bar{\boldsymbol{S}}_{\mathrm{k-1}}\|\boldsymbol{S}_{\mathrm{k}}) + 1. \end{aligned} \tag{12}$$

The period counts at k+2 instant can be predicted as

$$\begin{aligned} \boldsymbol{K}^{\mathrm{p}}_{\mathrm{u,k+2}} &= \boldsymbol{K}_{\mathrm{u,k+1}} + (\boldsymbol{S}_{\mathrm{k}}\|\bar{\boldsymbol{S}}^{\mathrm{p}}_{\mathrm{k+1}}), \\ \boldsymbol{K}^{\mathrm{p}}_{\mathrm{d,k+2}} &= \boldsymbol{K}_{\mathrm{d,k+1}} + (\bar{\boldsymbol{S}}_{\mathrm{k}}\|\boldsymbol{S}^{\mathrm{p}}_{\mathrm{k+1}}). \end{aligned} \tag{13}$$

Actual up and down switching periods in second, i.e., $\boldsymbol{T}_{\mathrm{u}} = (t_{\mathrm{u,a}}, t_{\mathrm{u,b}}, t_{\mathrm{u,c}})^\top$, $\boldsymbol{T}_{\mathrm{d}} = (t_{\mathrm{d,a}}, t_{\mathrm{d,b}}, t_{\mathrm{d,c}})^\top$, can be obtained using the period counts,

$$\boldsymbol{T}_{\mathrm{u,k}} = (\boldsymbol{T}_{\mathrm{u,k-1}} - T_{\mathrm{s}}\boldsymbol{Q}_{\mathrm{u,k}})(\boldsymbol{S}_{\mathrm{k-1}}\|\bar{\boldsymbol{S}}_{\mathrm{k}}) + T_{\mathrm{s}}\boldsymbol{Q}_{\mathrm{u,k}}, \tag{14}$$

$$\boldsymbol{T}_{\mathrm{d,k}} = (\boldsymbol{T}_{\mathrm{d,k-1}} - T_{\mathrm{s}}\boldsymbol{Q}_{\mathrm{d,k}})(\boldsymbol{S}_{\mathrm{k-1}}\|\bar{\boldsymbol{S}}_{\mathrm{k}}) + T_{\mathrm{s}}\boldsymbol{Q}_{\mathrm{u,k}}. \tag{15}$$

TABLE I
SYSTEM CONFIGURATION.

Parameters	Values
DC-link voltage V_{d} (V)	700
PMSM inductance $L_{\mathrm{s}}^{\mathrm{d}}$=$L_{\mathrm{s}}^{\mathrm{q}}$ (H)	19.43×10^{-3}
PMSM resistance R_{s} (Ω)	0.1379
PM Flux ψ_{pm} (Wb)	0.42675
PMSM Pole Pairs p (-)	3
PMSM Inertia J ($\mathrm{kg \cdot m^2}$)	0.01
Nominal Torque/Current $\mathrm{T_e^n/I_m^n}$ (Nm/A)	29/15
Rated speed ω_{m} (r/min)	1200
Sampling Time f_{s} (kHz)	80
Ref. switching frquency f_{sw}^{*} (kHz)	5
Weight factors $\lambda_{\mathrm{s}}, \lambda_{\mathrm{K}}$	0.2, 0.05

Switching frequency is the inverse of the switching period, obtained as [13],

$$f_{\mathrm{sw,k}} = \left(\frac{\|\boldsymbol{T}_{\mathrm{u,k}}\|_1 + \|\boldsymbol{T}_{\mathrm{d,k}}\|_1}{6} \right)^{-1}. \tag{16}$$

This frequency measurement mechanism enables us to update the switching frequency in every control period, which makes the f_{sw} control visualized and easier.

C. Mode switch criteria

Both speed reference changes and load torque variations lead to the transient operation of the drive system. The former is detected by the difference between the reference and the measured mechanical speed. The latter is distinguished by the variation of the measured speed, as shown below.

$$\Delta\omega = |\omega_{\mathrm{m,k}}^{*} - \omega_{\mathrm{m,k}}|, \ \Delta T = |\omega_{\mathrm{m,k}} - \omega_{\mathrm{m,k-1}}|, \tag{17}$$

Furthermore, we introduce the operating criterion J_{cri} to capture the variations of both the speed reference and the load torque,

$$J_{\mathrm{cri}} = \Delta\omega + \Delta T. \tag{18}$$

To overcome the chattering problem and improve the robustness of the mode selection, a hysteresis band is employed [17] (see Fig. 1c). If J_{cri} is larger than J_{H}, it means that the motor is in the transient stage and CDMPC is used. If J_{cri} is smaller than J_{L}, it means that the motor is in the steady stage and PPC is applied. When J_{cri} is between J_{L} and J_{H}, the control law does not change. Through this mechanism, a smooth transition between two control methods can be applied without chattering.

IV. SIMULATION RESULTS

In this section, the transient performances of classical DMPC and the PPC approach are compared, showing that classical DMPC has superior dynamics. In addition, overall control performance of the proposed switched DMPC is given; it achieves a fixed switching frequency with guaranteed control dynamics.

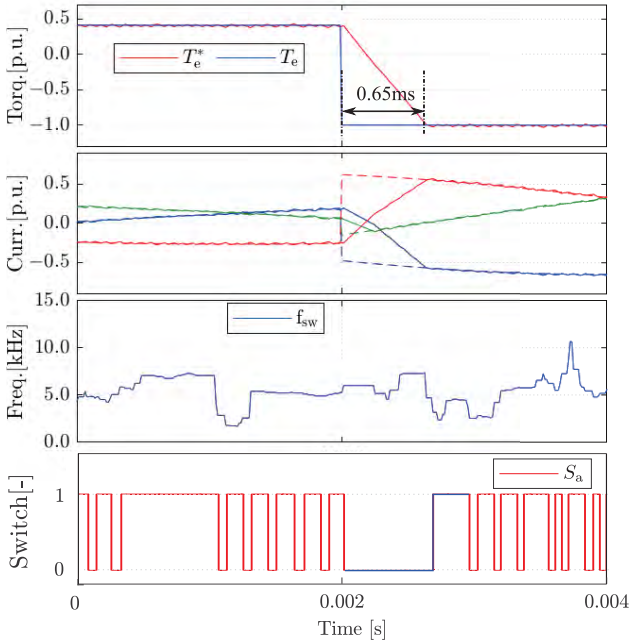

(a) Transient performance of CDMPC, with $\lambda_{\mathrm{s}} = 0.09$ to achieve $f_{\mathrm{sw}} \approx$ 5kHz.

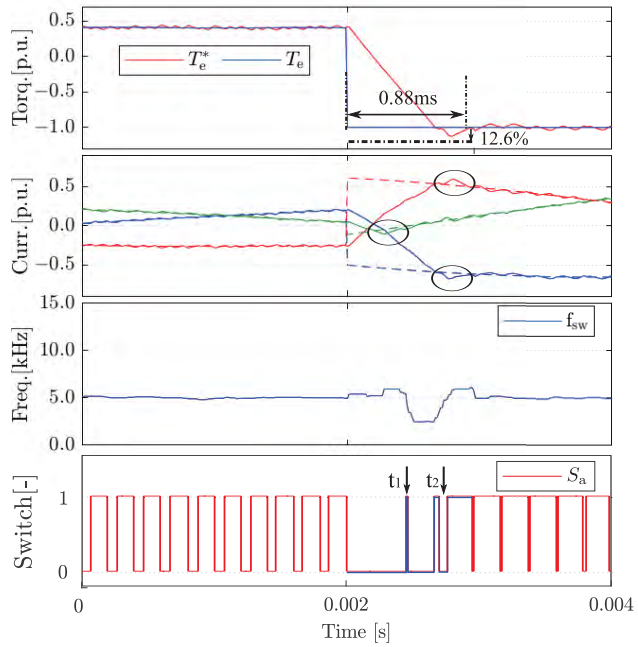

(b) Transient performance of PPC, with $f_{\mathrm{sw}}^{*} = 5$kHz.

Fig. 5. Transient performance comparison between classical DMPC and predictive period control approach. For each figure, from top to bottom are electromagnetic torque and its reference, three phase stator currents and their references, three phase switch positions and measured switching frequency. Note that, $T_{\mathrm{base}} = 25$Nm, $I_{\mathrm{base}} = 20$A.

A. Transient performance comparison between CDMPC and PPC

In the test scenario, the torque reference has a step change from 15Nm to -25Nm at 0.02s. As expected, CDMPC shows fast dynamics, taking 0.65ms to reach steady-state. However,

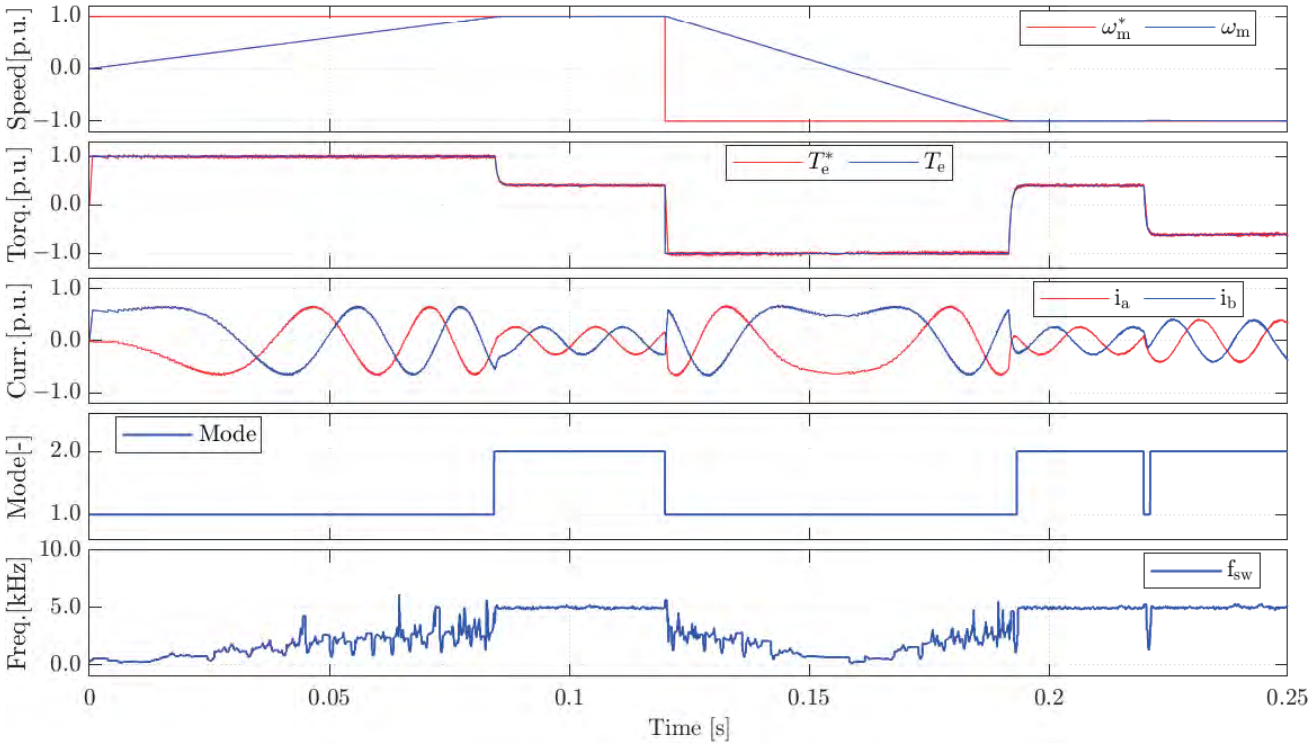

Fig. 6. Overall performance of switched DMPC. From up to down are mechanical speed and its reference, electromagnetic torque and its reference, stator currents, operating mode (1 for transient operation using CDMPC, 2 for steady-state operation using PPC), and measured switching frequency. Note that, $\omega_{\text{base}} = 1200$r/min.

the corresponding switching frequency is unfixed due to the lack of modulation stage. For PPC, the switching frequency is fixed in steady-state. During transients, f_{sw} of the PCC fluctuates around 5kHz. Nevertheless, the settling time of PCC is longer, taking 0.88ms to reach steady-state. Meanwhile, it exhibits overshoot in torque (12.6%) and currents. In summary, CDMPC shows a good transient performance with an unfixed f_{sw} and PPC achieves a fixed f_{sw} with deteriorated transient performance. The above analysis leads us to combine CDMPC and PPC, i.e., the proposed switched DMPC.

During transients, $\boldsymbol{S}_{\text{a}} = \{0, 1\}$ is the optimal control action to accurately track the reference (see fourth column of Fig. 3.a, highlighted by blue). However, for PPC, the switching signal is $\boldsymbol{S}_{\text{a}} = \{0, 1, 0, 1, 0, 1\}$ (see Fig. 3b) during transients, which leads to the deteriorated transient performance. The reason behind this phenomenon is the added period regulation term J_{K}, which forces *unnecessary* switch commutations when K approaches or exceeds the K^* to fix the switching frequency.

B. Overall performance of Switched MPC

The test scenarios are as follows: at 0.12s, speed reference has a inverse change from 1200r/min to -1200r/min; at 0.22s, the load torque varies from 10Nm to -15Nm. As is shown, the proposed solution is effective at wide operation points. Good steady and transient performances are achieved. For operating mode switch (fourth graph of Fig. 6), 1 denotes transient operation and 2 represents steady-state operation. In mode 1, classical DMPC is employed, achieving fast dynamics. In mode 2, the PPC method is utilized and it regulates the switching frequency at 5kHz. By using the mode switch criteria with the hysteresis band given in Sec. III-C, a smooth switch between the two modes is achieved. Note that, the test scenarios include speed step from zero to nominal speed and speed reverse, resulting in long transient time with unfixed f_{sw}. In reality, the transient time is usually shorter, fixed f_{sw} is realized in most cases. Besides, for CDMPC, the f_{sw} is basically below 5k Hz. Fortunately, it's sufficient to realize the guaranteed control dynamics during transients. Switch losses could also be reduced at the same time.

C. Steady-state performance of Switched MPC with fixed switching frequency

In steady-state, the currents exhibits modulation-like spectrum under different load conditions, as shown in Fig. 7. The current THD is 4.78% when T_{L} = 10Nm and becomes 3.13% when T_{L} = -15Nm.

V. Conclusions

The predictive period control approach achieves a fixed switching frequency without the use of a modulator, making it a promising alternative. However, degrading transient performance is observed when PPC controls the PMSM drives. The reason behind this phenomenon is that the added switching frequency regulation term forces unnecessary switch transitions during transient operation to ensure a fixed f_{sw}. To address this problem, a switched DMPC is proposed.

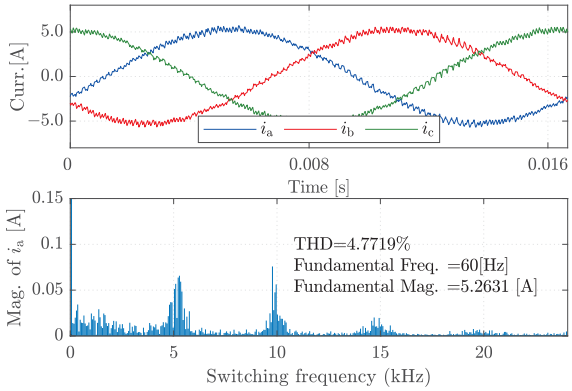

(a) FFT analysis of stator current when T_{L} is 10Nm.

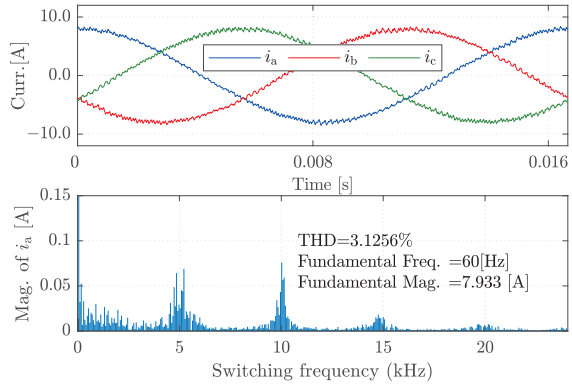

(b) FFT analysis of stator current when T_{L} is -15Nm.

Fig. 7. In steady-state, FFT analysis of stator current under different load conditions.

During transients, classical DMPC is used to guarantee control dynamics, while PPC is employed during steady-state and achieves fixed switching frequency. By virtue of the proposed mode switch criteria, a seamless switch is achieved between the two control laws. Future work will focus on reducing the high sampling frequency requirement of the PPC method.

REFERENCES

[1] S. Vazquez, J. I. Leon, L. G. Franquelo, J. Rodriguez, H. A. Young, A. Marquez, and P. Zanchetta, "Model Predictive Control: A Review of Its Applications in Power Electronics," *IEEE Industrial Electronics Magazine*, vol. 8, no. 1, pp. 16–31, 2014.

[2] P. Karamanakos and T. Geyer, "Guidelines for the Design of Finite Control Set Model Predictive Controllers," *IEEE Transactions on Power Electronics*, vol. 35, no. 7, pp. 7434–7450, 2020.

[3] X. Gao, S. Member, M. Abdelrahem, C. M. Hackl, and S. Member, "Direct Predictive Speed Control With a Sliding Manifold Term for PMSM Drives," *IEEE Journal of Emerging and Selected Topics in Power Electronics*, vol. PP, no. c, p. 1, 2019.

[4] P. Karamanakos, R. Mattila, and T. Geyer, "Fixed switching frequency direct model predictive control based on output current gradients," *Proceedings: IECON 2018 - 44th Annual Conference of the IEEE Industrial Electronics Society*, pp. 2329–2334, 2018.

[5] A. Mora, F. Donoso, M. Urrutia, A. Angulo, and R. Cardenas, "Predictive Control Strategy for an Induction Machine fed by a 3L-NPC Converter with Fixed Switching Frequency and Improved Tracking Error," in *2018 IEEE 27th International Symposium on Industrial Electronics (ISIE), Cairns, QLD*, 2018, pp. 155–160.

[6] M. Tomlinson, H. D. T. Mouton, R. Kennel, and P. Stolze, "A Fixed Switching Frequency Scheme for Finite-Control-Set Model Predictive Control-Concept and Algorithm," *IEEE Transactions on Industrial Electronics*, vol. 63, no. 12, pp. 7662–7670, 2016.

[7] F. Donoso, A. Mora, R. Cárdenas, A. Angulo, D. Sáez, and M. Rivera, "Finite-Set Model-Predictive Control Strategies for a 3L-NPC Inverter Operating With Fixed Switching Frequency," *IEEE Transactions on Industrial Electronics*, vol. 65, no. 5, pp. 3954–3965, 2018.

[8] A. Mora, R. Cardenas-Dobson, R. P. Aguilera, A. Angulo, F. Donoso, and J. Rodriguez, "Computationally Efficient Cascaded Optimal Switching Sequence MPC for Grid-Connected Three-Level NPC Converters," *IEEE Transactions on Power Electronics*, vol. 34, no. March, pp. 1–1, 2019.

[9] T. Geyer, *Model predictive control of high power converters and industrial drives*. John Wiley & Sons, 2016.

[10] P. Cortés, J. Rodríguez, D. E. Quevedo, and C. Silva, "Predictive current control strategy with imposed load current spectrum," *IEEE Transactions on power Electronics*, vol. 23, no. 2, pp. 612–618, 2008.

[11] C. A. Rojas, M. Aguirre, S. Kouro, T. Geyer, and E. Gutierrez, "Leakage Current Mitigation in Photovoltaic String Inverter Using Predictive Control With Fixed Average Switching Frequency," *IEEE Transactions on Industrial Electronics*, vol. 64, no. 12, pp. 9344–9354, 2017.

[12] M. Aguirre, S. Kouro, C. A. Rojas, J. Rodriguez, and J. I. Leon, "Switching Frequency Regulation for FCS-MPC Based on a Period Control Approach," *IEEE Transactions on Industrial Electronics*, vol. 65, no. 7, pp. 5764–5773, 2018.

[13] M. Aguirre, S. Kouro, C. A. Rojas, and S. Vazquez, "Enhanced Switching Frequency Control in FCS-MPC for Power Converters," *IEEE Transactions on Industrial Electronics*, vol. 0046, no. c, pp. 1–1, 2020.

[14] M. G. Eftekhar, Z. Ouyang, M. A. E. Andersen, P. B. Andersen, L. A. d. S. Ribeiro, and E. Schaltz, "Efficiency Study of Vertical Distance Variations in Wireless Power Transfer for E-Mobility," *IEEE Transactions on Magnetics*, vol. 52, no. 7, pp. 1–4, 2016.

[15] Z. Zhang, "On control of grid-tied back-to-back power converters and pmsg wind turbine systems," Ph.D. dissertation, Technical University of Munich, Germany, 2016.

[16] P. Cortes, J. Rodriguez, C. Silva, and A. Flores, "Delay compensation in model predictive current control of a three-phase inverter," *IEEE Transactions on Industrial Electronics*, vol. 59, no. 2, pp. 1323–1325, 2012.

[17] R. P. Aguilera, P. Lezana, and D. E. Quevedo, "Switched Model Predictive Control for Improved Transient and Steady-State Performance," *IEEE Transactions on Industrial Informatics*, vol. 11, no. 4, pp. 968–977, 2015.